THE LOCATION OF PHOTOPIGMENT MOLECULES IN THE CROSS-SECTION OF FROG RETINAL RECEPTOR DISK MEMBRANES

J. K. BLASIE

From the Department of Biophysics and Physical Biochemistry, Johnson Research Foundation, University of Pennsylvania, Philadelphia, Pennsylvania 19104

ABSTRACT The location of the photopigment molecules relative to the lipid hydrocarbon core of retinal receptor disk membranes was unknown. The photopigment molecules could occur entirely on the surface of the membrane, completely embedded in its hydrocarbon core, or at some intermediate location protruding into both the aqueous surface layer and the lipid core of the disk membrane. To resolve this uncertainty, we collected X-ray intensity data diffracted by the photopigment molecules in wet pellets of oriented frog retinal receptor disk membranes as a function of the electron density of the sedimentation medium. These data were fitted to a model which predicted the integrated intensity diffracted from the photopigment molecules as a function of the electron density of the sedimentation medium and the extent to which the molecule protruded into the aqueous surface layer and the lipid core of the disk membrane. This analysis showed that for the photopigment molecular diameter of ~42 A, about 28 A protrudes into the aqueous layer, and about 14 A into the lipid core for unbleached photopigment. Bleaching causes the photopigment to "sink" into the lipid core some 7 A. The partial embedding of the photopigment molecules in the lipid core introduces a correlation of the photopigment molecules with lipid hydrocarbon chains in the plane of the disk membranes.

1. INTRODUCTION

In earlier papers (1, 2) we identified the photopigment molecules and described their planar arrangement in wet isolated frog retinal receptor disk membranes. These studies provided no information about the location of the photopigment molecules in the cross-section of the disk membranes except for the fact that the aqueous negative stain phosphotungstate provided contrast for the photopigment molecules, allowing their observation by electron microscopy. Since the diameter of the photopigment molecules in the plane of the disk membrane was nearly identical as determined by electron microscopy vs. X-ray diffraction, it might appear that at least

half of the photopigment molecule projects into the aqueous surface layer of the disk membrane penetrated by the negative stain.

X-ray diffraction studies on intact frog retinal rods (3, 4) indicate that the disk membranes contain a lipid hydrocarbon core within their cross-section. Since detergents are required to extract photopigment from the disk membranes (5), the photopigment molecules are presumably directly associated with these lipid molecules forming the lipid core for the disk membrane.

These results suggest that the photopigment molecules occur in the cross-section of the disk membrane at an interface between the lipid hydrocarbon core and an aqueous surface layer. The photopigment molecules may presumably be embedded to some unknown extent in both the surface layer and the hydrocarbon core. The extent of this embedding has not been indicated by the cross-sectional electron density profiles for the disk membranes by previous work (3, 4) because (*a*) the location of the photopigment molecules has not been determined in these profiles, and (*b*) the thickness of the lipid hydrocarbon core as suggested by these profiles may be only an apparent thickness, depending on the extent of this embedding.

The experiments described in this paper determined the extent of the embedding of the photopigment molecules in the aqueous surface layer and lipid hydrocarbon core of the disk membrane as well as changes in this embedding induced by light absorption by the photopigment molecules. These studies make use of the idea that the electron density contrast between the sedimentation medium and that portion of the photopigment molecules which protrude into the aqueous surface layer of the disk membrane will affect the total diffraction arising from the photopigment molecules in a predictable way, depending on this contrast and the degree to which the molecules protrude into that aqueous phase.

This work has been reported briefly elsewhere.[1]

2. MATERIALS AND METHODS

Frog (*Rana pipiens*) retinal receptor disk membranes were isolated in dim red light in a manner similar to that previously described (1, 2). The disk membranes were collected from an interface separating 45% sucrose from a solution identical with the final sedimentation medium. The isolated disk membranes were then diluted 20:1 with the final sedimentation medium and pelleted at 68,000 *g* for 1 hr at 4°C in a specially designed Lucite cell with a cylindrical cavity 3 mm in diameter, sealed at the bottom with a Melinex window, giving a pellet 2–3 mm in thickness. If the photopigment was to be bleached, the disk membranes were bleached in white light just before this final sedimentation. The final sedimentation medium consisted of 0.01 M phosphate buffer, pH 7.5, with varying amounts of glucose, LiCl, or CsCl to adjust the electron density of the sedimentation medium to a desired value. The media used for this purpose were 0.25 M, 0.50 M, and 1.00 M glucose and 0.15 M LiCl and 0.15 M CsCl, all phosphate buffered as above.

The resulting pellet of wet disk membranes, either unbleached or bleached, was then mounted and sealed in a specimen chamber which allowed the X-ray beam incident along

[1] J. K. Blasie. 1970. *Biophys. Soc. Annu. Meet. Abstr.* **10**:51a.

the sedimentation axis while the wet pellet was maintained with 1 mm of sedimentation medium covering the pellet at 5 ±0.2°C for the duration of the exposure (15 hr) in all cases, and in darkness if the photopigment was not bleached.

The diffraction camera used was similar to that previously described (1, 2). The specimen-to-film distance was 62.5 mm in helium in all cases. The camera with cylindrical film cassette provided a low-angle resolution of 200 A to a high-angle resolution of 2 A. The camera used provided a line-focus source with a 1 mm height at the specimen. This height, together with the ±3% accuracy in the intensity measurement in the low-angle region as judged by the noise level in microdensitometer tracings of the diffraction patterns, allowed slit corrections to be neglected as previously discussed (2). Background scattering for this camera and these specimens was determined over angular range used ($0.005\ A^{-1} \leq 2 \sin \theta/\lambda \leq 0.500\ A^{-1}$) for Ni-filtered CuK$\alpha$ radiation and was subtracted from the microdensitometer tracings.

The diffracted intensities corrected for background were used for the calculations in section 4. The diffraction theory for these calculations appears in section 4. All nontrivial computations were performed on a PDP-6 computer (Medical School Computer Facility, University of Pennsylvania).

3. RESULTS

We have shown in earlier papers (1, 2) that X-ray diffraction from wet ultracentrifugal pellets of isolated frog retinal receptor disk membranes is cylindrically symmetric about the sedimentation axis. With the beam incident along the sedimentation axis, the beam is incident normal to the planes of the disk membranes and we obtain diffraction arising from electron density contrast projected in the plane of the disk membrane. X-ray diffraction obtained with the beam incident normal to the sedimentation axis arises from electron density contrast in the direction normal to the planes of the disk membranes providing reflections from the lamellar disk-to-disk repeat.

Fig. 1 shows diffraction obtained with the beam incident along the sedimentation axis from a disk membrane pellet in phosphate-buffered LiCl. For cylindrical coordinates r, ϕ, z for the disk membrane where z is normal to the disk membrane, the corresponding reciprocal space coordinates are r^*, ϕ^*, z^* with $\mathbf{z}\cdot\mathbf{z}^*/|\mathbf{z}||\mathbf{z}^*| = 1$. With the disk membrane pellet in this orientation with respect to the beam, we obtain the diffracted intensity $I(r^*, z^* = 0)$ defined here as $I_{obs}(r^*)$ where $r^* = 2 \sin \theta/\lambda$. We have previously shown that the intensity maxima for

$$r^* < 1/40\ A = r_0^*$$

arise from the planar arrangement of the photopigment molecules, i.e., the correlation of photopigment molecules with each other in the plane of the disk membrane. The diffracted intensity in this region is denoted by $i_{pp}(r^*)$ and $g_{pp}(\bar{\sigma}_m)$ is given by:

$$g_{pp}(\bar{\sigma}_m) = \int_0^{r_0^*} 2\pi r^* i_{pp}(r^*, \bar{\sigma}_m)\, dr^*,$$

where $\bar{\sigma}_m$ is the electron density of the sedimentation medium.

The intensity maximum at $r^* = 1/4.5$ A most likely arises from the correlation of phospholipid hydrocarbon chains with each other in the lipid hydrocarbon core (3, 4) in the plane of the disk membrane. This seems likely because (*a*) disk membranes have a lipid hydrocarbon core, and polarized light studies (6) indicate that the lipid hydrocarbon chains have an average orientation normal to the plane of the disk membrane, and (*b*) phospholipid-water systems regularly show a maximum at nearly identical diffraction angles which arises from the correlation of the hydrocarbon chains with each other (7).

Since changes in the electron density of the sedimentation medium would not be expected to alter electron density contrast for the lipid hydrocarbon chains in the core of the disk membrane, the integrated intensity $\mathcal{I}_{pp}(\bar{\sigma}_m)$ data for the photopigment molecules for different values of $\bar{\sigma}_m$ were scaled together, relative to the integrated intensity of the maximum at $r^* = 1/4.5$ A. The integrated intensity data $\mathcal{I}_{pp}(\bar{\sigma}_m)$ scaled in this manner for unbleached photopigment at five different values of $\bar{\sigma}_m$ and for bleached photopigment at three different values for $\bar{\sigma}_m$ are shown in Fig. 2. The error in the $\mathcal{I}_{pp}(\bar{\sigma}_m)$ values is $\pm 10\%$ allowing for both measurement errors in the diffracted intensities and scaling errors.

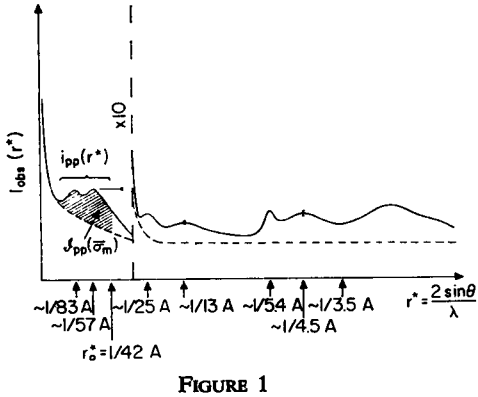

FIGURE 1

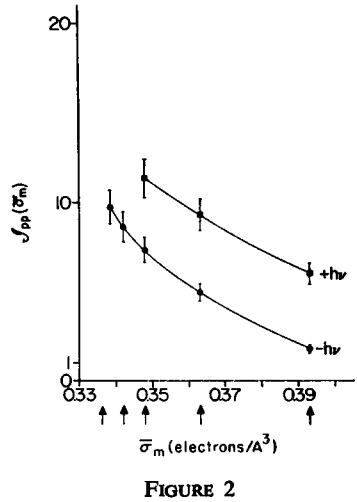

FIGURE 2

FIGURE 1 Diffracted X-ray intensity $I_{obs}(r^*)$ obtained from a wet pellet of disk membranes in buffered LiCl with the beam incident along the sedimentation axis. Background scattering for our cameras and these specimens is indicated by the dashed curve. Measurement errors in the observed diffracted intensity are indicated by the error bars and were regularly $\pm 3\%$ for $r^* \leq r_0^*$ and $\pm 8\%$ for $r^* > r_0^*$ as judged by the noise level in the microdensitometer tracings after correction for background.

FIGURE 2 Observed integrated X-ray intensity $\mathcal{I}_{pp}(\bar{\sigma}_m)$ diffracted by the photopigment molecules in wet disk membranes as a function of the electron density of the sedimentation medium $\bar{\sigma}_m$ and of bleaching of the photopigment. $\mathcal{I}_{pp}$ is indicated in Fig. 1 for the case of buffered LiCl. Errors in the integrated intensities are about $\pm 10\%$ allowing for both measurement and scaling errors and are indicated by error bars.

It is clearly seen that increasing the electron density of the sedimentation medium decreases the integrated diffracted intensity from the photopigment molecules relative to that from the lipid hydrocarbon chains for both unbleached and bleached photopigment. In addition, the integrated diffracted intensity from the photopigment molecules increases relative to that from the lipid hydrocarbon chains when the photopigment is bleached for all $\bar{\sigma}_m$ values investigated. We utilize the integrated intensity $\mathcal{I}_{pp}(\bar{\sigma}_m)$ here since these values are to be compared with the values calculated from theory presented in the next section.

The intensity maxima in the neighborhood of $r^* = 1/25$ A and $1/13$ A will be discussed in section 5. The maximum at $r^* = 1/5.4$ A will not be discussed at this time, and the maxima for $r^* \geq 1/3.5$ A arise from the sedimentation medium, i.e., water.

4. INTERPRETATION

In order to interpret these results, we first consider the following model with reference to Fig. 3 for the relationship of the photopigment molecules to the lipid hydrocarbon core of the disk membranes. We consider the photopigment molecules to be approximately spherical with uniform electron density and to occur at an interface separating the aqueous surface layer of the disk membrane and the lipid hydrocarbon core of the disk membrane. Justification for such a model is as follows: (*a*) the photopigment molecule should be nearly spherical if its molecular weight is ~28,000 (8) and its radius in the plane of the disk membrane is ~22 A (2); (*b*) the photopigment molecule may be considered as a sphere of uniform electron density for $r^* \leq 1/40$ A (2); (*c*) the disk membrane most likely has a lipid hydrocarbon core (3, 4),

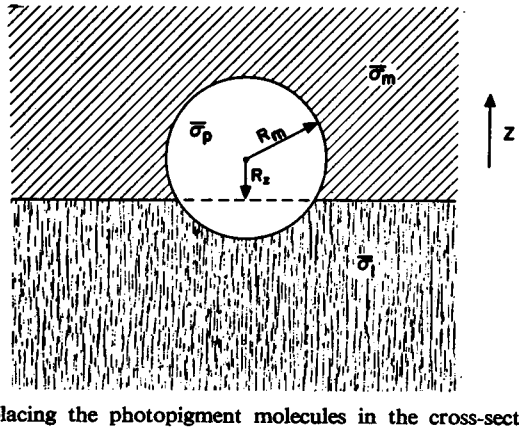

FIGURE 3 Model placing the photopigment molecules in the cross-section of the disk membrane at an interface separating an aqueous phase with average electron density $\bar{\sigma}_m$ and a lipid hydrocarbon phase with average electron density $\bar{\sigma}_l$. z is the direction normal to the membrane surface, R_m is the approximately spherical photopigment molecule's radius, $\bar{\sigma}_p$ is the average electron density of the photopigment molecule, and R_z determines the embedding of the photopigment molecule in each of the two membrane phases.

and reasons for considering the photopigment molecules to be embedded at such an interface were given in section 1; (*d*) the concentration of photopigment in retinal rods (9), its density, and that of adsorbed antirhodopsin in the plane of the disk membrane (1, 2), together with the amount of disk membrane in the retinal rod (3, 9), indicate that the photopigment molecules probably occur on only one side of the disk membranes, which is the side facing the sedimentation medium in pellets of isolated disk membranes (10); and (*e*) the sedimentation medium mainly provides electron density contrast for that portion of the photopigment molecule which protrudes into the aqueous surface layer of the disk membrane because any other nonphotopigment protein which occurs on the surface of the disk membrane must not be densely packed since the planar arrangement of the photopigment molecules is easily altered by temperature (2), pH, and ionic strength of the sedimentation medium (11), and, as will be shown in this paper, small ions and molecules as large as sucrose penetrate this aqueous surface layer to the same apparent extent.[2]

In our model, $(\bar{\sigma}_p - \bar{\sigma}_l)$ is the electron density contrast for that portion of the photopigment molecule occurring in the lipid hydrocarbon core of the disk membrane (where $\bar{\sigma}_p$ and $\bar{\sigma}_l$ are the average electron densities of the photopigment molecule and lipid hydrocarbon core, respectively, in electrons per cubic angstrom). $(\bar{\sigma}_p - \bar{\sigma}_m)$ is the electron density contrast for that portion of the photopigment molecule which protrudes into the aqueous surface layer of the disk membrane. For the radius of the photopigment molecule R_m, the parameter R_z determines the unknown extent to which the photopigment molecule is embedded in each of the two phases where R_z may lie in the range $-R_m \leq R_z \leq +R_m$. For example, if $R_z = -R_m$, the photopigment would occur entirely in the aqueous surface layer of the disk membrane and, for $R_z = +R_m$, it would occur entirely in the lipid hydrocarbon core of the disk membrane.

In order to determine the embedding parameter R_z from the integrated intensity data $\mathcal{I}_{pp}(\bar{\sigma}_m)$ in the previous section, we must extend the diffraction theory we used in an earlier paper (2). For a planar arrangement of hard spheres (*p*-particles) occurring *in vacuo*, we derived (equation 8, reference 2):

$$[i_{pp}(r^*)]_v = f_{p,v}^2(r^*) \cdot \Sigma^2(r^*), \tag{1}$$

where $[i_{pp}(r^*)]_v$ is the diffracted intensity from the hard spheres *in vacuo*, $f_{p,v}(r^*) \overset{s}{\rightleftharpoons} \sigma_p(r)$ where $\overset{s}{\rightleftharpoons}$ denotes the spherically symmetrical Fourier transform and $\sigma_p(r)$ is the electron density distribution for the *p*-particles where $\sigma_p(r) = \bar{\sigma}_p$, $r \leq R_m$, or 0, $r > R_m$, and $\Sigma(r^*) \overset{c}{\rightleftharpoons} \psi_p(r)$ where $\overset{c}{\rightleftharpoons}$ denotes the Fourier-Bessel

[2] We note that the interface in this model is operational in the sense that it is determined by the extent of penetration of small ions and small molecules into this aqueous surface layer of the disk membrane. However, since we will show that small monovalent cations and sucrose molecules penetrate this surface layer to the same depth and since, under this circumstance, the small monovalent cations would be expected to penetrate the surface layer to the nonpolar lipid hydrocarbon core of the disk membrane, this operational interface is most likely that described by the model.

transform and $\psi_p(r)$ is the planar distribution function for the hard spheres. For the same hard spheres embedded in a medium of a near-continuum of electron density of $\bar{\sigma}$, we derived (equation 9, reference 2):

$$[i_{pp}(r^*)]_{\bar{\sigma}} = \left(1 - \frac{\bar{\sigma}}{\bar{\sigma}_p}\right)^2 \cdot f^2_{p,v}(r^*) \cdot \Sigma^2(r^*), \tag{2}$$

where $[i_{pp}(r^*)]_{\bar{\sigma}}$ is the diffracted intensity from the hard spheres embedded in the medium. We note that equation 2 may be written:

$$[i_{pp}(r^*)]_{\bar{\sigma}} = f^2_{p,\bar{\sigma}}(r^*) \cdot \Sigma^2(r^*), \tag{3}$$

where

$$f_{p,\bar{\sigma}}(r^*) \rightleftharpoons \{\sigma_p(r) - \bar{\sigma}\}.$$

Using Parseval's theorem, we derived (equation 15, reference 2):

$$\int_0^{r_0^*} 2\pi r^* [i_{pp}(r^*)]_v \, dr^* = N \int_0^{\infty} 2\pi r \sigma_p^2(r) \, dr$$

$$= N \int_0^{r_0^*} 2\pi r^* f^2_{p,v}(r^*) \, dr^*, \tag{4}$$

where N is the number of coherently diffracting hard spheres. In an analogous fashion, we see that:

$$\int_0^{r_0^*} 2\pi r^* [i_{pp}(r^*)]_{\bar{\sigma}} \, dr^* = N \int_0^{r_0^*} 2\pi r^* f^2_{p,\bar{\sigma}}(r^*) \, dr^*. \tag{5}$$

For

$$[i_{pp}(r^*)]_{\bar{\sigma}} = K_{\bar{\sigma}} [i_{pp}(r^* > 0)]'_{\bar{\sigma}} + [i_{pp}(r^* = 0)]_{\bar{\sigma}},$$

where $[i_{pp}(r^*)]'_{\bar{\sigma}}$ is the observed diffracted intensity from the hard spheres on a relative scale, $K_{\bar{\sigma}}$ normalizes the relative intensities to the p-particle scattering factor $f_{p,\bar{\sigma}}(r^*)$ in the medium (in contrast to that used previously in equation 17, reference 2, which normalized the observed intensities to the scattering factor *in vacuo*), and $[i_{pp}(r^* = 0)]_{\bar{\sigma}}$ is the unobserved zero-angle diffraction where:

$$[i_{pp}(r^* = 0)]_{\bar{\sigma}} = N^2 f^2_{p,\bar{\sigma}}(r^* = 0).$$

Then we obtain from equation 5:

$$K_{\bar{\sigma}} \int_0^{r_0^*} 2\pi r^* [i_{pp}(r^* > 0)]'_{\bar{\sigma}} \, dr^* = N \int_0^{r_0^*} 2\pi r^* f^2_{p,\bar{\sigma}}(r^*) \, dr^* - \frac{N^2 f^2_{p,\bar{\sigma}}(r^* = 0)}{A}, \tag{6}$$

where A is the area in the plane available to the N hard spheres. From equation 6 we obtain in abbreviated form:

$$K_{\bar{\sigma}}/N = (B_{\bar{\sigma}} - C_{\bar{\sigma}}/A_0)/D_{\bar{\sigma}}.$$

From equation 3 and the definition of $f_{p,\bar{\sigma}}(r^*)$, it is apparent that this $K_{\bar{\sigma}}$ is independent of $\bar{\sigma}$ and $A_0 = A/N \simeq 4900\ \text{A}^2$ (2).

Now, for two different electron densities of the medium, $\bar{\sigma}_1$ and $\bar{\sigma}_2$, we have from equation 6:

$$D_{\bar{\sigma}_1}/D_{\bar{\sigma}_2} = (B_{\bar{\sigma}_1} - C_{\bar{\sigma}_1}/A_0)/(B_{\bar{\sigma}_2} - C_{\bar{\sigma}_2}/A_0). \tag{7}$$

To extend this result to our model for photopigment molecules in the disk membrane is relatively simple. The hard spheres are embedded at the interface between two media of average electron density $\bar{\sigma}_m$ and $\bar{\sigma}_l$ and the extent of the embedding in either medium is set by R_z. $f^2_{p,\bar{\sigma}_m}(r^*)$ is formed by setting up the Fourier transform of σ_p in cylindrical coordinates in the $z^* = 0$ projection with the origin at the center of the hard sphere and the z-axis normal to the plane of the interface. The integration in the z-direction uses $(\bar{\sigma}_p - \bar{\sigma}_l)$ as the electron density contrast for $-R_m \leq z \leq R_z$ and $(\bar{\sigma}_p - \bar{\sigma}_m)$ as the electron density contrast for $R_z \leq z \leq +R_m$:

$$f_{p,\bar{\sigma}_m}(r^*, R_z) = (\bar{\sigma}_p - \bar{\sigma}_l)\int_{-R_m}^{R_z} 2\pi(R_m^2 - z^2)\frac{J_1(2\pi r^*[R_m^2 - z^2]^{1/2})}{(2\pi r^*[R_m^2 - z^2]^{1/2})}\,dz + (\bar{\sigma}_p - \bar{\sigma}_m)\int_{R_z}^{R_m} 2\pi(R_m^2 - z^2)\frac{J_1(2\pi r^*[R_m^2 - z^2]^{1/2})}{(2\pi r^*[R_m^2 - z^2]^{1/2})}\,dz, \tag{8}$$

where J_1 is the first-order Bessel function arising from the integral over r and ϕ. The normalization constant for the observed diffracted intensity is again independent of $\bar{\sigma}_m$ since $\bar{\sigma}_m$ affects $[i_{pp}(r^* > 0)]'_{\sigma_m}$ and $f^2_{p,\bar{\sigma}_m}(r^*, R_z)$ in exactly the same manner and we obtain for two different values of $\bar{\sigma}_{m1}$ and $\bar{\sigma}_{m2}$:

$$D_{\bar{\sigma}_{m1}}/D_{\bar{\sigma}_{m2}} = (B_{\bar{\sigma}_{m1}} - C_{\bar{\sigma}_{m1}}/A_0)/(B_{\bar{\sigma}_{m2}} - C_{\bar{\sigma}_{m2}}/A_0). \tag{9}$$

Noting that $D_{\bar{\sigma}_m} = \mathcal{I}_{pp}(\bar{\sigma}_m)$ of the previous section, we see that ratios of the experimental pairs of $\mathcal{I}_{pp}(\bar{\sigma}_{m1})/\mathcal{I}_{pp}(\bar{\sigma}_{m2})$ may determine R_z knowing $\bar{\sigma}_{m1}$, $\bar{\sigma}_{m2}$ and assuming $\bar{\sigma}_p$, $\bar{\sigma}_l$ by varying R_z in the range $-R_m \leq R_z \leq +R_m$ until the right-hand side of equation 9 matches the experimentally determined left-hand side. Thus, the data for unbleached photopigment given in Fig. 2 provide 15 experimental pairs for determining R_z.

For a molecular weight for the photopigment of ~28,000 and molecular diameter of 42 A, $\bar{\sigma}_p \simeq 0.40$ electrons/A^3 and $\bar{\sigma}_l \simeq 0.28$ electrons/A^3 (3), we calculated

$$K_{\bar{\sigma}_m} \cdot D_{\bar{\sigma}_m}/N = (B_{\bar{\sigma}_m} - C_{\bar{\sigma}_m}/A_0), \tag{10}$$

for $R_m = 21$ A, $-R_m \leq R_z \leq +R_m$ at 1 A intervals of R_z, and 0.32 electrons/A^3 $\leq \bar{\sigma}_m \leq$ 0.50 electrons/A^3 at intervals of 0.002 electrons/A^3. A few of these curves are shown in Fig. 4.

For the experimental values of $\bar{\sigma}_m$ used in the previous section, we found that for unbleached photopigment, the 15 experimental ratios of $\mathcal{J}_{pp}(\bar{\sigma}_{mi}):\mathcal{J}_{pp}(\bar{\sigma}_{mj})$ all fit the curve for $R_z = -7 \pm 3$ A and for bleached photopigment, the three experimental ratios fit the curve $R_z = 0 \pm 3$ A, allowing for errors in the experimental ratios of the integrated intensities, as shown in Fig. 5. That is to say that for unbleached photopigment, the 15 experimental ratios fit the curves -10 A $\leq R_z \leq -4$ A and not the curves for $R_z \geq -3$ A or $R_z \leq -11$ A when experimental error was allowed for. We note that the R_z value determined from the LiCl vs. CsCl inte-

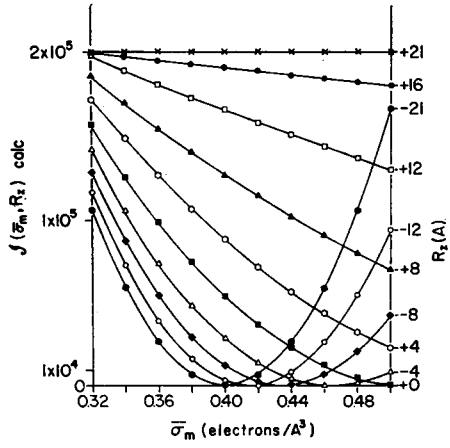

FIGURE 4 Calculated integrated X-ray intensity $\mathcal{J}(\bar{\sigma}_m, R_z)$ calc for the photopigment molecules in the model disk membrane shown in Fig. 3 as a function of the electron density of the sedimentation medium and the embedding parameter R_z. $\mathcal{J}(\bar{\sigma}_m, R_z)$ calc was calculated according to the right-hand side of equation 10.

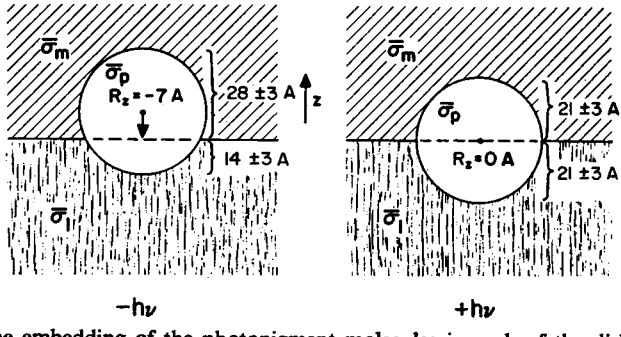

FIGURE 5 The embedding of the photopigment molecules in each of the disk membrane phases before and after bleaching of the photopigment as determined by a quantitative comparison of the data shown in Fig. 3 with the calculated integrated intensities $\mathcal{J}(\bar{\sigma}_m, R_z)$ calc shown in Fig. 4.

grated intensity data was $R_s = -8$ A while that for the three glucose concentrations gave $R_s = -7$ A (all for unbleached photopigment); i.e., they were identical within experimental error. In addition, the glucose data for unbleached and bleached photopigment provide an independent check on the R_s values for the two cases through the ratios of the three pairs $g_{pp}(\bar{\sigma}_{mi}, +h\nu)/g_{pp}(\bar{\sigma}_{mi}, -h\nu)$. This independent check is in good agreement with the previously determined values of $R_s(-h\nu) = -7 \pm 3$ A; $R_s(+h\nu) = 0 \pm 3$ A.

5. DISCUSSION

On the basis of these experiments, unbleached photopigment molecules with a molecular diameter of ~42 A protrude about 28 A into the aqueous surface layer of the disk membrane and are embedded in the lipid hydrocarbon core of the disk membranes to an extent of about 14 A, as shown in Fig. 5. After the photopigment is bleached, the protrusion of the photopigment molecule into the aqueous surface layer decreases to about 21 A, while the extent of its embedding in the lipid hydrocarbon core increases to about 21 A. Total bleaching of the photopigment molecules results in their sinking into the lipid hydrocarbon core of the disk membrane by about 7 A or approximately 16–17% of their molecular diameter. Unfortunately, exposure times required for these experiments prevent us from determining at what intermediate stage of the bleaching process this sinking occurs, but experiments described in another paper (11), together with these experiments, shed some light on this matter, and discussion of the problem is presented in that paper.

An alternative explanation for effect of bleaching on the integrated intensity data from the photopigment molecules presented in section 3 might appear to be that the average electron density of the photopigment molecule increases with bleaching. This explanation is unacceptable for two reasons: (*a*) the radius of the photopigment molecule is constant to within an accuracy of ±1 A on bleaching of the photopigment (11), and (*b*) if this were the case, the integrated intensity data for bleached photopigment would have a greater slope as a function of $\bar{\sigma}_m$ than that for the unbleached photopigment; the opposite is true for the data shown in Fig. 2.

We note that the "pure" lipid hydrocarbon region indicated in the derived cross-sectional electron density distribution for disk membranes is about 20 A (3, 4). The fact that we have shown that the photopigment molecules are embedded in lipid hydrocarbon some 21 A after bleaching need not indicate that the photopigment molecule spans the thickness of the hydrocarbon core. The electron density level of this ~20 A-thick low electron density region in the disk membrane's cross-section is most likely that of nearly pure lipid hydrocarbon (3). Since the density of photopigment in the plane of the disk membrane is sufficient to significantly raise the electron density of the hydrocarbon core penetrated by the photopigment over that of pure lipid hydrocarbon, this ~20-A-thick low electron density region is mostly

unpenetrated by the photopigment. Thus, the total thickness occupied by lipid hydrocarbon in the disk membrane's cross-section is roughly 40 A, the sum of the pure hydrocarbon region and that penetrated by the photopigment.

There are two important implications from the results of this determination of the location of the photopigment molecules relative to the lipid hydrocarbon core of the disk membrane. The first is that one might expect that the surface of the photopigment molecule which protrudes into the aqueous surface layer of the disk membrane is composed primarily of polar residues. These polar residues might give the photopigment molecules net electric charge. This electric charge would be expected to influence the planar arrangement of the photopigment molecules. A reorganization of this electric charge distribution resulting in a change in the area occupied on the surface of the photopigment molecule by these polar residues would affect the extent of the embedding of the photopigment molecules in the lipid hydrocarbon core of the disk membrane. Evidence supporting this implication is reported in another paper (11).

The second implication arises since the embedding of the photopigment molecules in the lipid hydrocarbon core of the disk membrane is to an extent of approximately half of their molecular diameter. This situation suggests that diffraction may arise from the correlation of photopigment molecules with phospholipid hydrocarbon chains in the plane of the disk membrane. Since the molecular radius of the photopigment molecule is about 21 A, and the radius of a lipid hydrocarbon chain is about 2.25 A (7), the distance of closest approach for the photopigment molecules and the lipid hydrocarbon chains would be about 23 A, which could give rise to diffraction in the region $r^* \geq 1/30$ A. Since diffraction is observed in this region from the disk membranes (Fig. 1), we decided to see if this observed diffraction could arise from such an intercorrelation of photopigment molecules and lipid hydrocarbon chains in the plane of the disk membrane.

In order to do this, we consider the following simplified model. We suppose the photopigment molecules to be hard spheres embedded in a planar arrangement of hard cylinders where the cylinder axis is normal to the plane and the cylinders represent the lipid hydrocarbon chains whose average orientation is normal to the plane of the disk membrane (6). We then obtain for the electron density distribution for this model structure:

$$\rho(\mathbf{r}) = \sigma_p(\mathbf{r}) * \psi_p(r) + \sigma_l(\mathbf{r}) * \psi_l(r), \tag{11}$$

for usual cylindrical coordinates r, ϕ, z, where σ_p and σ_l are the electron density distribution for the hard sphere and hard cylinder, respectively, and ψ_p and ψ_l are the planar distribution functions for the hard spheres and hard cylinders, respectively. For the diffracted intensity from such a system for the usual cylindrical coordinates with the beam incident normal to the plane of the arrangement of spheres

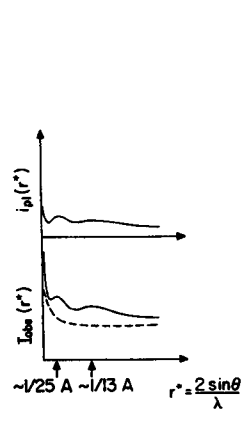

FIGURE 6

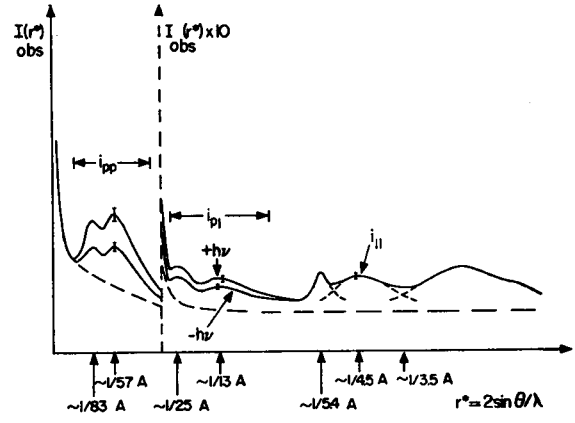

FIGURE 7

FIGURE 6 Calculated diffracted intensity arising from a random correlation of photopigment molecules with lipid hydrocarbon chains in the plane of the disk membrane i_{pl} (r^*), compared with I_{obs} (r^*) in the region $1/30 \text{ A} \leq r^* \leq 1/7$ A.

FIGURE 7 The dependence of the observed diffracted intensity arising from the correlation of photopigment molecules with lipid hydrocarbon chains in the plane of the disk membrane, i_{pl} (r^*), on photopigment bleaching. i_{pp}, i_{pl}, i_{ll} are considered to be the first, second, and third terms in equation 10, respectively. Errors due to measurement and scaling are indicated by the error bars.

and cylinders, i.e. the $z^* = 0$ projection, it is not difficult to show that:[3]

$$I_{obs}(r^* > 0) \propto N_p f_p^2(r^*)[1 + h_{pp}(r^*)] + 2(N_p N_l)^{1/2} f_p(r^*) f_l(r^*) h_{pl}(r^*) + N_l f_l^2(r^*([1 + h_{ll}(r^*)]. \quad (12)$$

For our purpose here, we need consider only the second term, $i_{pl}(r^* > 0)$, in equation 12, the diffracted intensity arising from the correlation of the spheres with the cylinders in the plane. To see the functional form of the calculated $i_{pl}(r^* > 0)$, we take the radius R_p of the p-spheres as 21 A, the radius R_l of the l-cylinders as

[3] where N_p and N_l are the relative numbers of the p-spheres and l-cylinders,

$$f_p(r^*) \overset{s}{\rightleftharpoons} \sigma_p(\mathbf{r}), f_l(r^*) = f_l(r^*, z^* = 0) \overset{c}{\rightleftharpoons} \sigma_l(\mathbf{r}), \rho_p(g_{pp}(r) - 1) \overset{c}{\rightleftharpoons} h_{pp}(r^*),$$

$$\rho_l(g_{ll}(r) - 1) \overset{c}{\rightleftharpoons} h_{ll}(r^*), (\rho_p\rho_l)^{1/2} g_{pl}(r) \overset{c}{\rightleftharpoons} h_{pl}(r^*), \rho_p = N_p/A, \rho_l = N_l/A,$$

where A is the area total available to the system of spheres and cylinders, and

$$\psi_p(r) * \psi_p(-r) = N_p\delta(r) + N_p(N_p - 1) g_{pp}(r), \psi_p(r) * \psi_l(-r) = N_p N_l g_{pl}(r),$$

$$\psi_l(r) * \psi_l(-r) = N_l\delta(r) + N_l(N_l - 1) g_{ll}(r).$$

$*$ is the convolution symbol, and $I(\mathbf{r}^*) \rightleftharpoons \rho(\mathbf{r}) * \rho(-\mathbf{r})$, where $\mathbf{r}$ and $\mathbf{r}^*$ are the general real and reciprocal space vectors.

2.25 A, and we assume that the correlation of p-spheres with the l-cylinders is random in the plane, i.e., the pair correlation function

$$g_{pl}(r) = \begin{cases} 0, r \leq (R_p + R_l) \\ 1, r > (R_p + R_l), \text{ where } (R_p + R_l) \end{cases}$$

is the distance of closest approach of the l-cylinders to the p-spheres. The functional form of the resulting calculated $i_{pl}(r^* > 0)$ is compared in Fig. 6 with $I_{obs}(r^*)$ shown in Fig. 1 for $1/30$ A $\leq r^* \leq 1/7$ A where both intensities have been scaled together for $1/10$ A $\leq r^* \leq 1/7$ A.

We note that both the calculated and observed intensity in this angular range have maxima of similar shape, relative magnitude, and position, indicating that the observed diffraction could arise from such a random correlation of photopigment molecules and lipid hydrocarbon chains in the plane of the disk membrane. In addition, bleaching the photopigment increases both of these observed maxima relative to the $r^* = 1/4.5$ A maxima, as shown in Fig. 7. This may be expected if the photopigment molecules are correlated with lipid hydrocarbon chains in the plane of the disk membrane, and the photopigment is embedded to a greater extent in these hydrocarbon chains when bleached.

6. CONCLUSIONS

Analysis of integrated X-ray intensity diffracted by the photopigment molecules in wet pellets of isolated frog retinal receptor disk membranes as a function of the electron density of the sedimentation medium indicates the following:

(*a*) The nearly spherical photopigment molecules ~42 A in diameter occur at an interface separating the lipid hydrocarbon core and the aqueous surface layer of the disk membrane protruding about 28 A into the aqueous phase and about 14 A into the lipid core.

(*b*) The photopigment molecules sink about 7 A when bleached, protruding approximately 21 A into both the aqueous surface layer and the lipid core.

(*c*) The portion of the photopigment molecule which is embedded in the lipid core may introduce a random correlation of the photopigment molecules with the lipid hydrocarbon chains in the plane of the disk membrane

This work was supported by United States Public Health Service grant GM12202.

Received for publication 18 August 1970 and in revised form 2 March 1971.

REFERENCES

1. BLASIE, J. K., C. R. WORTHINGTON, and M. M. DEWEY. 1969. *J. Mol. Biol.* 39:407.
2. BLASIE, J. K., and C. R. WORTHINGTON. 1969. *J. Mol. Biol.* 39:417.
3. GRAS, W. J., and C. R. WORTHINGTON. 1969. *Proc. Nat. Acad. Sci. U.S.A.* 63(2):233.
4. BLAUROCK, A. E., and M. H. F. WILKINS. 1969. *Nature (London).* 223:906.

5. HUBBARD, R. 1953. *J. Gen. Physiol.* **37**:381.
6. SCHMIDT, W. J. 1938. *Kolloid-Z.* **85**:137.
7. DERVICHIAN, D. G. 1964. *Progr. Biophys. Mol. Biol.* **14**:263.
8. HELLER, J. 1969. *Biochemistry.* **8**:675.
9. LIEBMAN, P. A. 1962. *Biophys. J.* **2**:161.
10. DEWEY, M. M., P. K. DAVIS, J. K. BLASIE, and L. BARR. 1969. *J. Mol. Biol.* **39**:395.
11. BLASIE, J. K. 1972. *Biophys. J.* **12**:205.